

1064 nm Dispersive Raman Micro-Spectroscopy and Optical Trapping of Pharmaceutical Aerosols

Peter J. Gallimore¹, Nick M. Davidson², Markus Kalberer¹, Francis D. Pope² and Andrew D. Ward^{3*}

¹ Department of Chemistry, University of Cambridge, Cambridge, CB2 1EW, U.K.

² School of Geography, Earth and Environmental Sciences, University of Birmingham, Birmingham, B15 2TT, U.K.

³ Central Laser Facility, Research Complex at Harwell, Rutherford Appleton Laboratory, Didcot, OX11 0FA, U.K.

ABSTRACT: Raman spectroscopy is a powerful tool for investigating chemical composition. Coupling Raman spectroscopy with optical microscopy (Raman micro-spectroscopy) and optical trapping (Raman Tweezers) allows microscopic length scales and hence femtolitre volumes to be probed. Raman micro-spectroscopy typically uses UV/visible excitation lasers, but many samples including organic molecules and complex tissue samples fluoresce strongly at these wavelengths. Here we report the development and application of dispersive Raman micro-spectroscopy designed around a near-infrared continuous wave 1064 nm excitation light source. We analyse micro-particles (1-5 μm diameter) composed of polystyrene latex and from three real-world pressurised metered dose inhalers (pMDIs) used in the treatment of asthma: salmeterol xinafoate (Serevent®), salbutamol sulfate (Salamol®), and ciclesonide (Alvesco®). For the first time, single particles are captured, optically levitated and analysed using the same 1064 nm laser, which permits a convenient non-destructive chemical analysis of the true aerosol phase. We show that particles exhibiting overwhelming fluorescence using a visible laser (514.5 nm) can be successfully analysed with 1064 nm excitation irrespective of sample composition and irradiation time. Spectra are acquired rapidly (1-5 min) with a wavelength resolution of 2 nm over a wide wavenumber range (500-3100 cm^{-1}). This is despite the microscopic sample size and low Raman scattering efficiency at 1064 nm. Spectra of individual pMDI particles compare well to bulk samples and the Serevent pMDI delivers the thermodynamically preferred crystal form of salmeterol xinafoate. 1064 nm dispersive Raman micro-spectroscopy is a promising technique which could see diverse applications for samples where fluorescence-free characterisation is required with high spatial resolution.

Raman spectroscopy provides a real time, non-invasive means to interrogate chemical composition. The wavelengths of light scattered by molecules provide information about the functional groups present, and in many cases a “molecular fingerprint” for a given structure¹.

Combining Raman spectroscopy with optical microscopy (Raman micro-spectroscopy) allows microscopic particles and droplets to be probed². However, to investigate microscopic samples without the use of immobilising substrates, which may perturb their equilibrium and kinetic properties, strategies to stably levitate single micron-sized particles have been developed^{3,4}. Raman micro-spectroscopy of optically trapped particles has been used to better understand cloud and aerosol chemistry in the atmosphere^{5,6} and processes occurring in single biological cells⁷. Typically the use of dispersive Raman microspectroscopy, rather than FT-Raman spectroscopy, is favoured in optical trapping applications where higher sensitivities and lower detector limits are beneficial in the analysis of single microparticles.

A recent application of particular interest is the characterisation of aerosol drugs from real-world medical inhalers⁸. Pressurised Metered Dose Inhalers (pMDIs) are an effective and rapid means of delivering pharmaceuticals to the lungs, and are the most commonly used delivery system for treating asthma, chronic obstructive pulmonary disease and other respiratory diseases⁹. Raman spectroscopy enables polymorphic crystal forms of drugs to be distinguished¹⁰, and the uptake of water vapour to be monitored on the particle’s journey from

inhaler to a high humidity “model lung”¹¹.

Since Raman scattering is a relatively weak process, applications of Raman spectroscopy typically employ high intensity incident radiation from visible, near-UV or near-IR lasers. However, many samples of interest contain organic functional groups which fluoresce over the detected wavelength range. Photochemistry caused by UV/visible excitation sources can also lead to the production of fluorescent photoproducts. If fluorophores are present, the high intensity laser can result in fluorescence which obscures and overwhelms Raman spectral features¹².

In general, shorter wavelength excitation is preferable for Raman spectroscopy because scattering is strongly wavelength dependent, scaling with λ^{-4} . However, autofluorescence also generally increases at shorter wavelengths due to increased fluorophore excitation. Recent studies have reported problematic fluorescence of pharmaceutical aerosols at a visible excitation wavelength (514.5 nm)^{8,11}. For biological tissue samples, which contain an abundant mixture of fluorophores, autofluorescence has been reported even in the near-IR (785 and 830 nm)^{13–15}. Sample substrates such as glass coverslips can also cause fluorescence¹³.

To overcome this problem in the current study, we perform Raman micro-spectroscopy using much lower photon energies from a 1064 nm excitation laser. This substantially reduces and in many cases entirely eliminates the possibility of fluorescence. Recent developments in detector technology facilitate dispersive Raman measurements at these longer wave-

lengths. Specifically we utilise an InGaAs array detector with quantum efficiency values exceeding 60% across a wavelength range of 950 nm to 1650 nm. 1064 nm dispersive Raman spectroscopy has been used to analyse liver tissue samples^{13–15} using a focal spot size of 25 μm , and living photolabile cells¹⁶ using a pulsed laser source (10 kHz repetition rate, 30 ns pulse width) with high peak powers. Here we use a continuous wave 1064 nm laser to both optically trap and interrogate single micron-sized particles: polystyrene beads used as laboratory standards, and real-world pharmaceutical aerosols from pMDIs. We first present spectra for particles collected onto coverslips and then substrate-free measurements on optically levitated aerosols.

EXPERIMENTAL SECTION

Aerosol environmental chamber and materials.

Particles were introduced into an environmental chamber for analysis. The chamber design has been reported previously^{11,17}. It consists of an aluminium cell with internal dimensions $10 \times 2 \times 1$ cm, with borosilicate glass windows at the top and bottom to transmit the optical trapping and Raman laser beams (described in section 2.2). The particle was illuminated using an LED source (Comar Optics) and an additional window on the side of the cell enabled brightfield imaging of the trapped particle using a CCD camera (Sony XC-ST51CE) coupled to an objective lens (Mitutoyo M Plan Apo 20 \times).

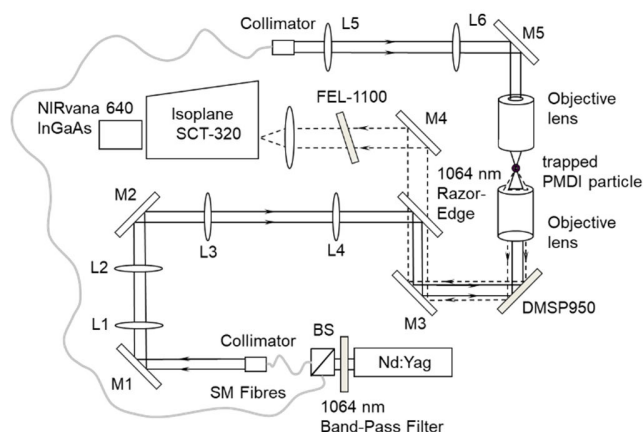


Figure 1. Optical setup for the 1064 nm dispersive Raman microscopy of optically trapped particles. L = lens, M = mirror, BS = beam splitter, SM = single mode.

The cell contains inlet and outlet ports connected to Teflon tubing (internal diameter 4 mm) to enable introduction of particles and gases. A series of commercially available pressurised metered dose inhalers (pMDIs) were used to generate pharmaceutical aerosols. Salbutamol sulfate (Salamol[®], Ivax), salmeterol xinafoate (Serevent[®], GlaxoSmithKline Group) and ciclesonide (Alvesco[®], Nycomed GmbH) pMDIs were connected to the chamber inlet tubing via a rubber septum. For optical trapping experiments, single particles (1–5 μm) were isolated and levitated in the optical trap following pMDI actuation. For coverslip experiments, particles were allowed to deposit onto the bottom coverslip following actuation. The cell was carefully cleaned between experiments using water and methanol (HPLC grade, Sigma). The outlet port was connected to an exhaust.

Polystyrene latex (PSL) spheres were also introduced to the

chamber via a custom-built atomiser. In addition to conventional PSL spheres (2.1 μm , Invitrogen, S37500, Lot 1129650), spheres containing the fluorescent dye Envy Green (3.87 μm , Bangs Laboratories, FS05F, Lot 10755) were used to demonstrate fluorescence during Raman spectrum acquisition in a controlled manner. Envy Green has a peak absorption wavelength of 525 nm and a peak emission wavelength of 565 nm. The fluorescent spheres were not atomised but diluted in water and a droplet placed on a clean coverslip prior to trapping a single bead in solution.

Relative humidity (RH) and temperature were continuously monitored via a probe inside the chamber (Sensiron SHT-75). Following particle introduction, the chamber RH was maintained below 5% using a continuous 0.2 L/min flow of dry nitrogen. Experiments were performed in an air-conditioned, temperature-controlled lab (20.5 $^{\circ}\text{C}$).

Counter-propagating dual beam optical trap. The optical trapping strategy has been described previously^{6,8,18} and is capable of stably levitating micron-sized solid and liquid particles (including those of non-spherical geometry) for hours-days. The trapping beams were generated using a continuous wave 1064 nm Nd:Yag laser (Ventus, Laser Quantum) passed through a beam splitter (Oz optics) and fibre-coupled into two single-mode fibres. The laser powers through the top and bottom objective lenses were 15 mW and 10 mW respectively. The foci of the lasers were positioned 10 μm apart to create a stable trapping volume for particles in the size range 1–5 μm .

Raman spectroscopy. Raman spectroscopy was performed with laser wavelengths of 514.5 nm and 1064 nm. The apparatus for 514.5 nm Raman spectroscopy has been discussed previously¹¹. For 1064 nm Raman spectroscopy, combined with optical trapping, a Nd:Yag laser (Laser Quantum, Ventus) was used with a measured maximum laser power of between 40 and 66 mW at the focus point of the objective lenses. The counter-propagating optical trap was configured as previously⁶ but with the modifications, shown in Figure 1, to the lower pathway. This reconfiguration, using high-quality optical components, was essential to maximise the NIR backscattered signal at the spectrograph. The laser beam was aligned through two sets of expansion optics (L1 to L4)¹⁹, reflected from a long-pass razor edge dichroic mirror (Semrock LPD01-1064) and directed through the objective lens with a dichroic mirror (Thorlabs, DMSP950). The second dichroic mirror allows the sample to be visualised under brightfield illumination with the laser wavelength blocked from the camera using a colour filter (Comar, KG5). However, during acquisition of a Raman spectrum the microscope illumination was blocked.

The Raman light scattered from the focal point was collected and collimated by the objective lens (Mitutoyo, Plan Apo NIR, x50 magnification, NA 0.42, working distance 17 mm) and directed back along the same optical pathway. An edge filter (Thorlabs, FEL 1100) was placed after the razor edge dichroic to transmit only the Raman shifted light above 1100 nm. The beam was then focussed through the entrance slit (width 100 μm) of a spectrograph (Acton Research Company, Isoplan SCT-320) and dispersed onto an InGaAs (640x512) array detector (Princeton Instruments, NIRvana 640, 20 μm pixels) with a 150 g/mm grating blazed at 1.2 μm . The spectral resolution for this configuration is stated by the manufacturer as 1.95 nm. Calibration of the spectrometer was performed using a Penray lamp (Hg) and verified by acquiring a Raman

spectrum from a sample vial of toluene (Aldrich, Spectroscopic grade). Recorded peak positions for toluene were accurate to 1.6 rel. cm^{-1} . No corrections were made to the spectral intensity other than background subtraction inherent in the Princeton Instruments' LightField 4 control software. The efficiency of the InGaAs array detector decreases above 1.5 μm such that the CH stretching region was of relatively low intensity.

The conditions for signal acquisition were as follows: For samples on cover slips the 1064 nm laser power was 50 mW as measured at focus and the spectra were collected for a total of 50 seconds for all pMDI formulations. For the Envoy Green fluorescent beads the power was 50 mW and the acquisition time was 10 seconds. For optically levitated pMDI particles of salbutamol sulfate and ciclesonide the total power was 40 mW and spectra acquired for 300 seconds. For optically trapping of salmeterol xinafoate the total power was 66 mW and spectra acquired for 140 seconds. For 514.5 nm Raman of the fluorescent beads sample, the laser power was 20 mW at focus, spectra acquired for 0.2 seconds, using a 30 μm slit width and a 600 g/mm grating blazed at 500 nm. The Serevent pMDI particles shown in Figure 2(b) were continuously acquired with an exposure time of 5 seconds per frame and 514.5 nm laser power of 4.3 mW at focus.

For the PSL and coverslip pMDI samples, 1064 nm spectra were acquired over three overlapping wavenumber ranges (266-1957, 1188-2579 and 2092-3211 cm^{-1}). Overlapping regions agreed well and were processed and averaged as described below to give the full spectra. Optically trapped pMDI spectra were acquired over the low wavenumber range (266-1957 cm^{-1}) only.

Data treatment. The intensity of Raman-scattered light is inherently weak, and the strong wavelength dependence (λ^{-4}) results in a factor of ~ 18 less signal at 1064 nm than 514.5 nm, so the 1064 nm spectra of single particles were processed post-acquisition. A Finite Impulse Response (FIR) filter was applied to the raw data using Mathematica v11 (Wolfram) using the Lowpass Filter function to remove high-frequency noise. Filtering is preferable to techniques such as Savitzky-Golay (SG) "smoothing" which effectively diminish spectral resolution²⁰. A comparison of the raw, FIR-filtered and SG-smoothed spectra is shown in Figure S1.

RESULTS AND DISCUSSION

Wavelength-dependent sample fluorescence. We exemplify the fluorescence problem described in the introduction in Figure 2. Figure 2(a) shows spectra of Envoy Green dyed polystyrene spheres acquired using 514.5 and 1064 nm excitation lasers. The Raman spectral features of the polystyrene are not even visible at 514.5 nm due to fluorescence from the dye. Envoy Green exhibits a broad emission maximum at 565 nm which corresponds to the broad peak around 1700 cm^{-1} in the spectrum. By contrast, a fluorescence-free spectrum is acquired at 1064 nm and compares well with literature reports of polystyrene beads²¹.

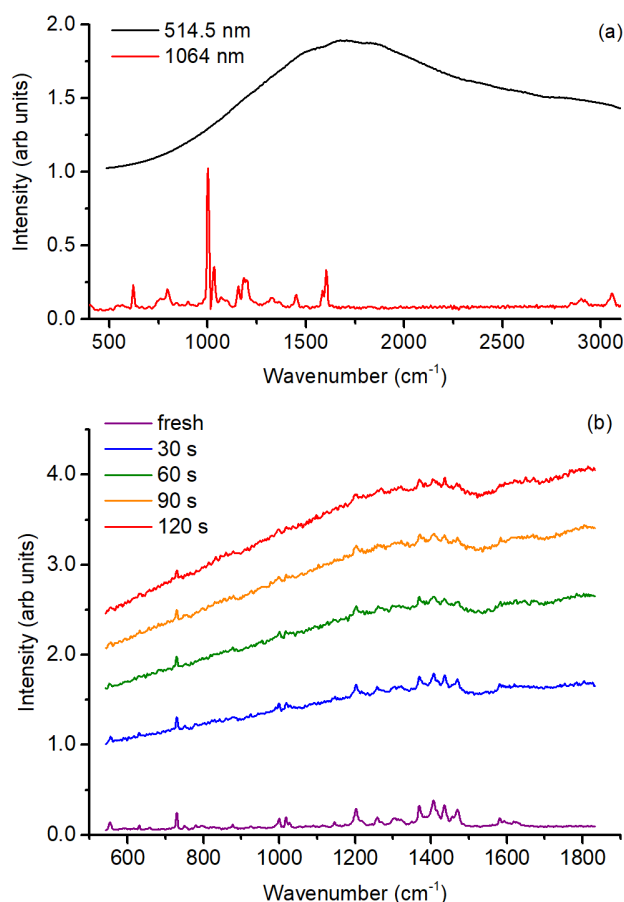


Figure 2. (a) Raman spectra of Envoy Green-dyed polystyrene beads using 514.5 and 1064 nm excitation lasers. The 514.5 nm spectrum is offset and scaled to aid comparison with the 1064 nm spectrum. Acquisition times were 0.2 and 10 s at 514.5 and 1064 nm respectively. The spectrum is overwhelmed by fluorescence at 514.5 nm, but free from fluorescence at 1064 nm. (b) Time-resolved Raman spectra of an optically trapped salmeterol xinafoate (Serevent) pMDI particle acquired using a 514.5 nm laser. Following exposure to the 514.5 nm laser, sample degradation rapidly causes fluorescence and the Raman spectral features are obscured within minutes. The spectrum background intensity increases over time due to fluorescence; the spectra are not deliberately offset as in (a).

Figure 2(b) shows spectra for the asthma drug salmeterol xinafoate, acquired following different exposure times to a 514.5 nm excitation laser. The spectrum initially resembles previous spectra reported in the literature¹⁰, but as noted in Davidson et al.¹¹, fluorescence commences almost immediately following irradiation by the visible laser due to the presence of the fluorophore in xinafoic acid. Since one of the key advantages of optical trapping techniques is the ability to interrogate single particles over long periods of time, photochemical sample degradation represents a major limitation for samples containing organic fluorophores.

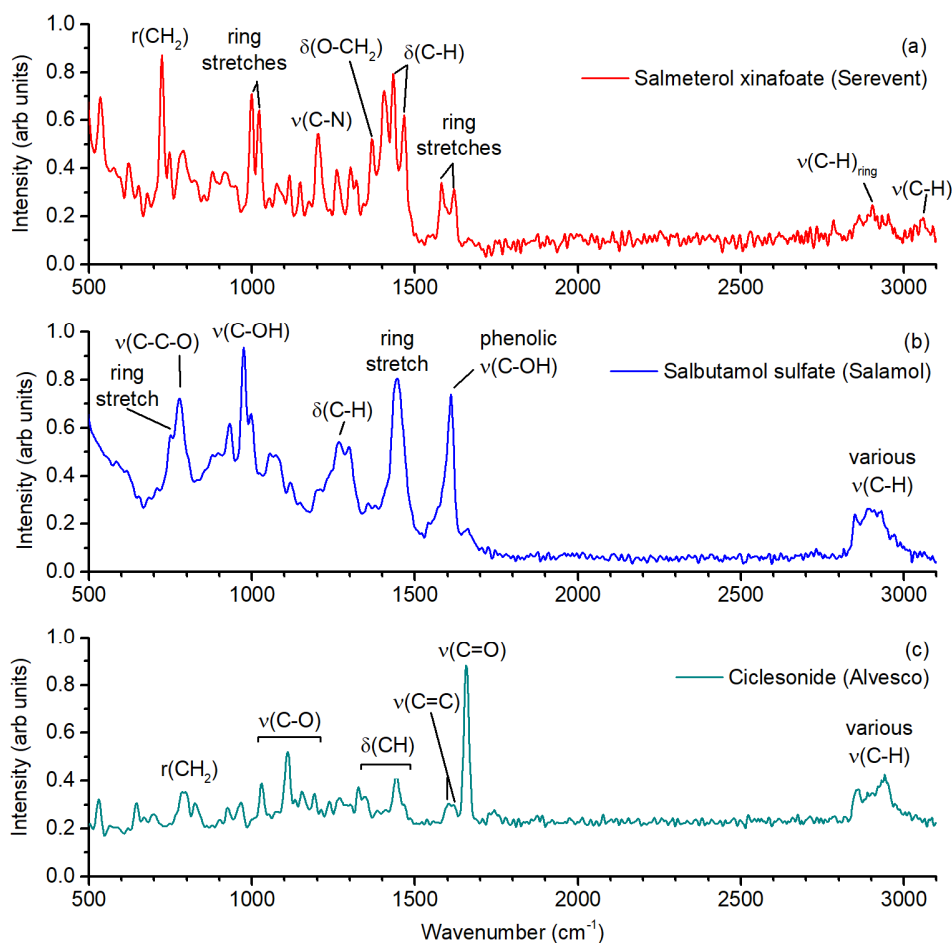


Figure 3. 1064 nm dispersive Raman spectra acquired for (a) salmeterol xinafoate (Serevent), (b) salbutamol sulfate (Salamol) and (c) ciclesonide (Alvesco) pMDI particles collected on the coverslip. None of the samples showed evidence of the fluorescence problems demonstrated using a 514.5 nm excitation laser (Figure 2 and Tong et al.⁸). Major peaks in each spectrum were assigned based on previous literature and the single-particle spectra here agree well with previous bulk samples.

pMDI particles collected on coverslip. For the remainder of the manuscript we exclusively use 1064 nm excitation to avoid fluorescence and photodegradation. We first report data from pharmaceutical particles collected onto a glass coverslip without the added technical complexity of optical trapping. This allows us to compare 1064 nm dispersive Raman spectra to previous literature, and assess the fluorescence characteristics of particles under these conditions. Raman spectra of salmeterol xinafoate, salbutamol sulfate and ciclesonide pMDI particles are shown in Figure 3.

Spectra obtained for all three pharmaceutical aerosols compare very well with previous literature and theoretical predictions^{10,11,22,23}. Major features for salmeterol xinafoate include ring stretches (1000, 1022, 1582 and 1620 cm^{-1}), an amine stretch (1204 cm^{-1}), a C-O bending mode (1369 cm^{-1}) and C-H bending modes (1432 and 1467 cm^{-1}). Salbutamol sulfate shows diagnostic peaks corresponding to C-C-O stretching (777 cm^{-1}), asymmetric hydroxyl group stretching (975 cm^{-1}), C-H bending (1261 cm^{-1}), ring stretching (1445 cm^{-1}) and a complex mode related to the phenolic hydroxyl group (1613 cm^{-1}). Ciclesonide exhibits a dominant peak at 1657 cm^{-1} corresponding to the α,β -unsaturated C=O and others related to C-O stretching (1112 cm^{-1}), C-H bending (1300-1470 cm^{-1})

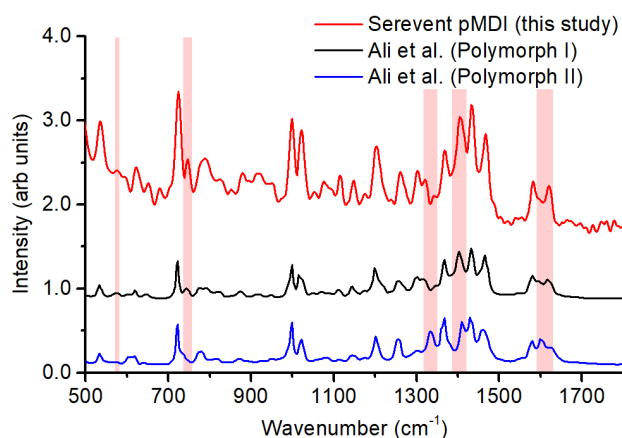


Figure 4. Comparison of 1064 nm Raman spectra for salmeterol xinafoate. Red: a single Serevent pMDI particle (this study). Blue and black: bulk powder spectra for two different polymorphs recorded by Ali et al.¹⁰. The pMDI particle is consistent with polymorph I, and several spectral features highlighting the differences between the two polymorphs are marked by shaded bands.

and C=C stretching ($1600\text{--}1620\text{ cm}^{-1}$). All three spectra show expected C-H stretching modes in the region $2850\text{--}3100\text{ cm}^{-1}$, although the intensity is diminished by reduced detection of NIR light at these wavelengths ($>1.5\text{ }\mu\text{m}$). A detailed assignment of all the spectra in Figure 3 is provided in Tables S1–S3.

The spectra for all three drugs were consistent irrespective of exposure to the 1064 nm laser, and no changes indicative of fluorescence could be observed following >1 hour of constant exposure. This is advantageous for several reasons: Firstly, single particles can in principle be monitored for long time periods, including in response to changes in environmental parameters such as relative humidity. Secondly, we have confirmed that use of this same 1064 nm laser for optical levitation (demonstrated below) is unlikely to cause sample degradation. Finally, longer spectrum integration times could be used as a means of compensating for the reduced Raman signal at longer wavelengths if required.

Raman spectra provide a sensitive probe not only of molecular structure but also crystal packing. Many crystalline drugs exhibit polymorphism, where several stable crystal structures can form depending on the conditions during crystal growth. Different polymorphs can exhibit differences in properties relevant to aerosol drug delivery such as crystal morphology and dissolution kinetics²⁴. Ali et al.¹⁰ reported spectra for two forms of salmeterol xinafoate as bulk powders and distinguished them via Raman spectral features. As here, they noted that near infrared laser excitation performed better than visible excitation in terms of avoiding background fluorescence and more clearly identifying and distinguishing the two crystal forms. All spectra acquired across a number of Serevent pMDI particles in this study match the spectrum for polymorph I as shown in Figure 4.

Characteristic peaks which distinguish the polymorphs are indicated on Figure 4. Peaks unique to polymorph I include the ring stretch band at 1405 cm^{-1} and the shoulder at 1597 cm^{-1} , the ring vibration bands at 1320 and 748 cm^{-1} , the C-H bending mode at 1346 cm^{-1} and the in-plane CCN bending mode at 578 cm^{-1} . Additionally, peaks expected for polymorph II, such as the C-H bending mode at 1338 cm^{-1} , are absent. Polymorph I is the most thermodynamically stable form at room temperature and pressure²⁵. We have shown here that it is also the form delivered by the Serevent pMDIs following manufacture and storage. Micro-spectroscopy of single particles may allow the stability and interconversion of polymorphs, and amorphous drug preparations, to be assessed with respect to environmental parameters such as relative humidity and temperature.

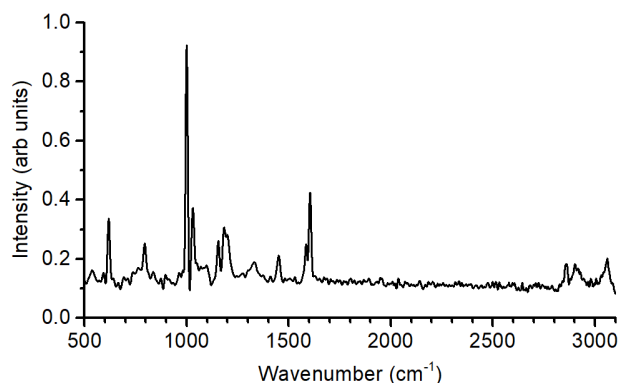


Figure 5. 1064 nm dispersive Raman spectrum for an optically trapped PSL particle.

Optically levitated particles. Levitation of particles enables unique observations which are not possible if the particle resides on the surface of a coverslip. A straightforward example is observation of native particle morphology (shape, phase separation, mixing state)²⁶. Other measurements become difficult to replicate for particles deposited on coverslips. For instance, dynamic environmental or physiological changes can cause airborne particles to take up a liquid phase (e.g. water), forming a core-shell particle or a solution droplet in the process. Coverslip measurements of these particles are complicated by factors such as capillary condensation, surface wettability and the contact angle of the liquid with the substrate. This

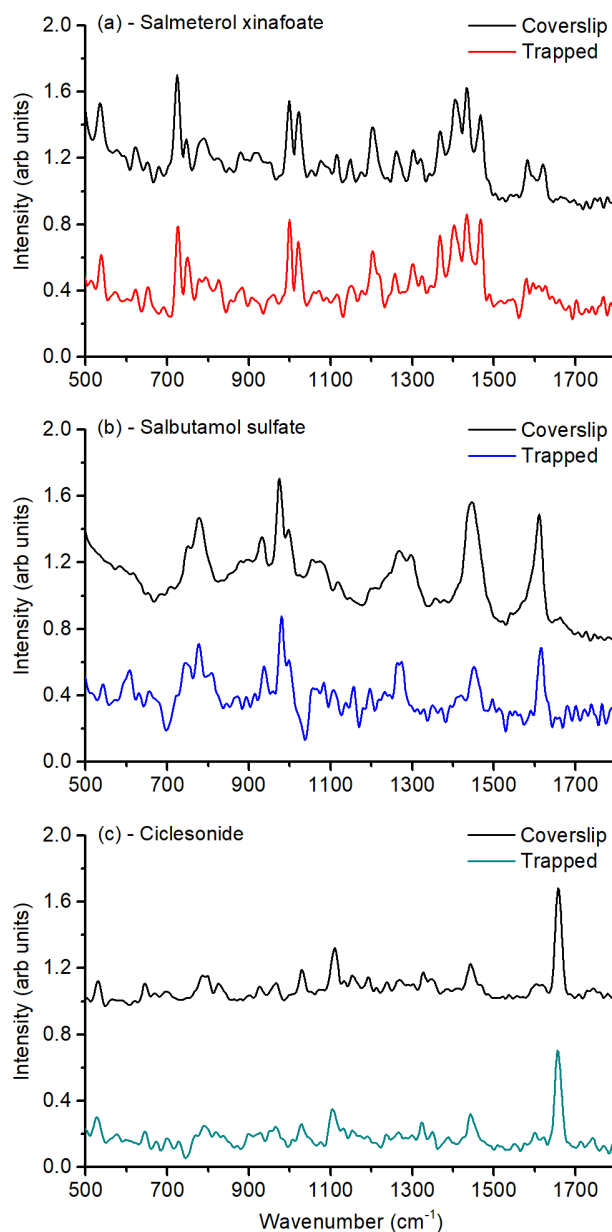


Figure 6. 1064 nm dispersive Raman spectra for optically trapped single particles of (a) salmeterol xinafoate, (b) salbutamol sulfate and (c) ciclesonide, from commercial pMDIs. Spectra for particles deposited on the coverslip (presented in Figure 3) are scaled and offset for comparison.

can cause unrealistic droplet morphologies to form, as demonstrated for salbutamol sulfate in Figure S2. Since such morphologies do not have the same surface area and internal capillary pressure as airborne particles, gas-particle equilibria (e.g. droplet water content), and the rates of dynamic processes, are modified in a non-trivial way.

Other studies have highlighted that deposition of particles on surfaces can result in additional artefacts^{27,28}, for instance because the surface acts as a nucleus for phase changes including crystallisation. This is particularly relevant for characterising pharmaceutical aerosols because, as discussed above, most drugs can exhibit multiple solid forms with different physico-chemical properties²⁹.

While technically more complex, acquisition of spectra in the true aerosol phase is therefore desirable. Here we demonstrate our unique ability to use the same near infrared laser for optical levitation and fluorescence-free spectrum acquisition. Figure 5 shows a spectrum for an optically trapped PSL particle over the full wavenumber range. The spectrum shows good agreement with previously reported spectra for optically trapped PSL particles²¹.

Spectra for optically trapped single pMDI particles are also shown, in Figure 6. We present spectra for all three pMDI drugs, and show the corresponding coverslip spectra presented in Figure 3 for reference. We focus on the region between 500–1800 cm⁻¹ where most of the diagnostic spectral features are present.

There is excellent agreement between the spectra acquired for optically trapped particles and those deposited on the coverslip in terms of peak positions and relative intensities. The spectra of optically trapped particles are slightly noisier than corresponding coverslip spectra (where generally larger particles were analysed than the upper particle size limit imposed by optical trapping). If required, this could be compensated for by longer integration times as discussed above. Nonetheless, we have provided a proof-of-principle demonstration here that characteristic spectra of single levitated aerosol particles (1–5 µm) can be obtained with a relatively short acquisition time and without any problematic fluorescence.

CONCLUSIONS

1064 nm dispersive Raman micro-spectroscopy has been successfully demonstrated for polystyrene latex (PSL) spheres and real-world pharmaceutical aerosols from pressurised metered dose inhalers (pMDIs). Spectra have been acquired for particles deposited on to a coverslip substrate and for single micron-sized particles stably levitated in an optical trap. The much lower photon energies associated with excitation at 1064 nm avoided sample fluorescence which is a common interference for materials such as organic solids, minerals and biological tissues at shorter wavelengths.

The strategy presented here probes small (femtolitre) volumes and since spectral acquisition is non-destructive, allows acquisition of a sequence of spectra over an extended period of time. It is therefore potentially applicable to a wide range of samples which are spatially heterogeneous (e.g. 2-dimensional “imaging” of biological tissues deposited on a coverslip) or which change over time (e.g. the response of an airborne particle to surface reactions or changes in environmental parameters).

ASSOCIATED CONTENT

Supporting Information

The Supporting Information is available free of charge on the ACS Publications website.

The supporting information contains discussion of spectrum processing techniques, an example of coverslip influence on particle morphology, and full assignments of the three pMDI Raman spectra shown in Figure 3.

AUTHOR INFORMATION

Corresponding Author

*E-mail: andy.ward@stfc.ac.uk

Author Contributions

ADW and FDP conceived the study. PJG, NMD and ADW performed the experiments. PJG and ADW analyzed the data. PJG wrote the manuscript. All authors assisted with manuscript preparation.

Notes

The authors declare no competing financial interest.

ACKNOWLEDGMENT

We thank Peter Seville for the provision of pMDI devices. This project was supported financially by the European Research Council (ERC), grant 279405, and the Science and Technology Facilities Council (STFC), Central Laser Facility Programme Access Grant (LSF1207).

REFERENCES

- (1) Smith, E.; Dent, G. *Modern Raman Spectroscopy - A Practical Approach*; John Wiley & Sons: Chichester, UK, 2005.
- (2) Puppels, G. J.; de Mul, F. F.; Otto, C.; Greve, J.; Robert-Nicoud, M.; Arndt-Jovin, D. J.; Jovin, T. M. Studying single living cells and chromosomes by confocal Raman microspectroscopy. *Nature* **1990**, *347*, 301–303.
- (3) Thurn, R.; Kiefer, W. Raman-Microsampling Technique Applying Optical Levitation by Radiation Pressure. *Appl. Spectrosc.* **1984**, *38*, 78–83.
- (4) Petrov, D. V. Raman spectroscopy of optically trapped particles. *J. Opt. A* **2007**, *9*, S139–S156 DOI: 10.1088/1464-4258/9/8/S06.
- (5) King, M. D.; Thompson, K. C.; Ward, A. D. Laser tweezers raman study of optically trapped aerosol droplets of seawater and oleic acid reacting with ozone: Implications for cloud-droplet properties. *J. Am. Chem. Soc.* **2004**, *126* (51), 16710–16711 DOI: 10.1021/ja044717o.
- (6) Rkiouak, L.; Tang, M. J.; Camp, J. C. J.; McGregor, J.; Watson, I. M.; Cox, R. A.; Kalberer, M.; Ward, A. D.; Pope, F. D. Optical trapping and Raman spectroscopy of solid particles. *Phys. Chem. Chem. Phys.* **2014**, *16*, 11426–11434 DOI: 10.1039/c4cp00994k.
- (7) Chan, J. W. Recent advances in laser tweezers Raman spectroscopy (LTRS) for label-free analysis of single cells. *J. Biophotonics* **2013**, *6* (1), 36–48 DOI: 10.1002/jbio.201200143.
- (8) Tong, H.-J.; Fitzgerald, C.; Gallimore, P. J.; Kalberer, M.; Kuimova, M. K.; Seville, P. C.; Ward, A. D.; Pope, F. D. Rapid interrogation of the physical and chemical characteristics of salbutamol sulphate aerosol from a pressurised metered-dose inhaler (pMDI). *Chem. Commun.* **2014**, *50*, 15499–15502 DOI: 10.1039/c4cc05803h.
- (9) Aggarwal, B.; Gogtay, J. Use of pressurized metered dose inhalers in patients with chronic obstructive pulmonary disease: review of evidence. *Expert Rev. Respir. Med.* **2014**, *8* (3), 349–356.
- (10) Ali, H. R. H.; Edwards, H. G. M.; Hargreaves, M. D.; Munshi, T.; Scowen, I. J.; Telford, R. J. Vibrational spectroscopic characterisation of salmeterol xinafoate polymorphs and a preliminary investigation of their transformation using

- simultaneous in situ portable Raman spectroscopy and differential scanning calorimetry. *Anal. Chim. Acta* **2008**, *620*, 103–112 DOI: 10.1016/j.aca.2008.05.009.
- (11) Davidson, N.; Tong, H.; Kalberer, M.; Seville, P. C.; Ward, A. D.; Kuimova, M. K.; Pope, F. D. Measurement of the Raman spectra and hygroscopicity of four pharmaceutical aerosols as they travel from pressurised metered dose inhalers (pMDI) to a model lung. *Int. J. Pharm.* **2017**, *520*, 59–69 DOI: 10.1016/j.ijpharm.2017.01.051.
 - (12) Chase, D. B. Fourier Transform Raman Spectroscopy. *J. Am. Chem. Soc.* **1986**, *40*, 7485–7488.
 - (13) Lieber, C. A.; Wu, H.; Yang, W. Tissue measurement using 1064 nm dispersive Raman spectroscopy. *Proc SPIE* **2014**, *8572* (12), 1–5 DOI: 10.1117/12.2008265.
 - (14) Patil, C. A.; Pence, I. J.; Lieber, C. A.; Mahadevan-Jansen, A. 1064nm dispersive Raman spectroscopy of tissues with strong near-infrared autofluorescence. *Opt. Lett.* **2014**, *39* (2), 303–306 DOI: 10.1364/OL.39.000303.
 - (15) Pence, I. J.; Patil, C. A.; Lieber, C. A.; Mahadevan-Jansen, A. Discrimination of liver malignancies with 1064 nm dispersive Raman spectroscopy. *Biomed. Opt. Express* **2015**, *6* (8), 2724–2737 DOI: 10.1364/BOE.6.002724.
 - (16) Ando, M.; Sugiura, M.; Hayashi, H.; Hamaguchi, H. 1064 nm Deep Near-Infrared (NIR) Excited Raman Microspectroscopy for Studying Photolabile Organisms. **2011**, *65* (5), 488–492 DOI: 10.1366/10-06196.
 - (17) Fitzgerald, C.; Hosny, N. A.; Tong, H.-J.; Seville, P. C.; Gallimore, P. J.; Davidson, N. M.; Athanasiadis, T.; Botchway, S. W.; Ward, A. D.; Kalberer, M.; et al. Fluorescence lifetime imaging of optically levitated aerosol: a technique to quantitatively map the viscosity of suspended aerosol particles. *Phys. Chem. Chem. Phys.* **2016**, *18*, 21710–21719 DOI: 10.1039/C6CP03674K.
 - (18) Jones, S. H.; King, M. D.; Ward, A. D. Atmospherically relevant core – shell aerosol studied using optical trapping and Mie scattering. *Chem. Commun.* **2015**, *51*, 4914–4917 DOI: 10.1039/C4CC09835H.
 - (19) Fallman, E.; Axner, O. Design for fully steerable dual-trap optical tweezers. *Appl. Opt.* **1997**, *36* (10), 2107–2113.
 - (20) Clupek, M.; Matejka, P.; Volka, K. Noise reduction in Raman spectra: Finite impulse response filtration versus Savitzky – Golay smoothing. *J. Raman Spectrosc.* **2007**, *38*, 1174–1179 DOI: 10.1002/jrs.
 - (21) Xie, C.; Dinno, M. A.; Li, Y. Near-infrared Raman spectroscopy of single optically trapped biological cells. **2002**, *27* (4), 249–251.
 - (22) Ali, H. R. H.; Edwards, H. G. M.; Kendrick, J.; Scowen, I. J. Vibrational spectroscopic study of salbutamol hemisulphate. *Drug Test. Anal.* **2009**, *1*, 51–56 DOI: 10.1002/dta.8.
 - (23) Feth, M. P.; Volz, J.; Hess, U.; Sturm, E.; Hummel, R.-P. Physicochemical, Crystallographic, Thermal and Spectroscopic Behavior of Crystalline and X-ray Amorphous Ciclesonide. *J. Pharm. Sci.* **2008**, *97* (9), 3765–3780 DOI: 10.1002/jps.21223.
 - (24) Blagden, N.; Matas, M. De; Gavan, P. T.; York, P. Crystal engineering of active pharmaceutical ingredients to improve solubility and dissolution rates. *Adv. Drug Deliv. Rev.* **2007**, *59*, 617–630 DOI: 10.1016/j.addr.2007.05.011.
 - (25) Tong, H. H. Y.; Shekunov, B. Y.; York, P.; Chow, A. H. L. Characterization of Two Polymorphs of Salmeterol Xinafoate Crystallized from Supercritical Fluids. **2001**, *18* (6), 852–858.
 - (26) Krieger, U. K.; Reid, J. P.; Krieger, U. K. Exploring the complexity of aerosol particle properties and processes using single particle techniques. *Chem. Sci.* **2012**, *41*, 6631–6662 DOI: 10.1039/c2cs35082c.
 - (27) Eom, H.; Gupta, D.; Li, X.; Jung, H.; Kim, H.; Ro, C. Influence of Collecting Substrates on the Characterization of Hygroscopic Properties of Inorganic Aerosol Particles. *Anal. Chem.* **2014**, *86*, 2648–2656 DOI: 10.1021/ac4042075.
 - (28) Shahidzadeh-Bonn, N.; Rafai, S.; Bonn, D.; Wegdam, G.; V, U. R. N.; Uni, V. Salt Crystallization during Evaporation: Impact of Interfacial Properties. *Langmuir* **2008**, *24*, 8599–8605.
 - (29) Lee, A. Y.; Erdemir, D.; Myerson, A. S. Crystal Polymorphism in Chemical Process Development. *Annu. Rev. Chem. Biomol. Eng.* **2011**, *2*, 259–280 DOI: 10.1146/annurev-chembioeng-061010-114224.

Insert Table of Contents artwork here:

